Industrial and Domestic Waste Management

Research Article
Volume 5(2), 2025, 182−194
https://doi.org/10.53623/idwm.v5i2.945

A Sustainable Sugarcane Bagasse Biochar–Bentonite Composite for Peroxide Value Reduction in Used Cooking Oil

Avissa Auryn Wijayanti[1], Adhi Yuniarto[1]*, Indah Nurhayati[2], Sagita Rochman[3]

[1]Department of Environmental Engineering, Faculty of Civil, Environmental and Geo Engineering, Institut Teknologi Sepuluh Nopember, Surabaya 60111, Indonesia
[2]Department of Environmental Engineering, Faculty of Engineering, Universitas PGRI Adi Buana Surabaya, Surabaya, 60234, Indonesia
[3]Department of Electrical Engineering, Faculty of Engineering, Universitas PGRI Adi Buana Surabaya, Surabaya, 60234, Indonesia

*Correspondence: adhy@its.ac.id

SUBMITTED: 4 December 2025; REVISED: 18 December 2025; ACCEPTED: 23 December 2025

ABSTRACT: Used cooking oil underwent thermal and oxidative degradation due to repeated heating, resulting in increased peroxide levels and producing rancid odors, discoloration, and potential toxicity. In this study, the initial peroxide value of the used cooking oil was 56.42 meq O_2/kg, indicating significant oxidative degradation. The study evaluated the ability of activated sugarcane bagasse-bentonite (ASBB) and non-activated (SBB) composites to reduce peroxide values. Characterization was performed using SEM-EDX and FTIR, while adsorption efficiency was tested by varying the adsorbent dose (2–10 g) and treatment time (0–180 minutes). Peroxide reduction was analyzed using iodometric titration. The results showed that ASBB was more effective, with 10 g of ASBB and 180 minutes of treatment reducing the peroxide value by up to 82.3–84.5%.

KEYWORDS: Used cooking oil; peroxide value; sugarcane bagasse; bentonite

1. Introduction

Used cooking oil referred to cooking oil that had undergone repeated use and heating, rendering it susceptible to thermal and oxidative degradation [1]. This degradation process induced alterations in the physical and chemical properties of the oil, including foam formation, the development of a rancid odor, a color change from bright yellow to brownish, and increased levels of free fatty acids and peroxide value [2]. The accumulation of peroxide value, resulting from the oxidation of unsaturated fatty acids at elevated temperatures, generated free radicals, hydroperoxides, and derivative compounds such as aldehydes and ketones [3, 4]. These compounds were toxic and posed significant health risks, including cardiovascular disease, neurological disorders, and an elevated risk of cancer due to cellular and DNA damage [5].

In addition to health implications, the improper disposal of used cooking oil presented substantial environmental challenges, leading to drainage blockages, water contamination, and degradation of soil and ecosystem vitality [6, 7]. Consequently, it was imperative to implement

circular economy strategies for the repurposing of waste cooking oil, one of which included a purification process aimed at reducing the concentration of harmful compounds such as peroxides. The peroxide value was the main parameter used to assess the oxidation level of used cooking oil and to determine its suitability for recycling as a feedstock for biodiesel [8].

Adsorption was a widely utilized purification method due to its effectiveness, cost efficiency, and environmental sustainability. The adsorption process enabled the removal of oxidative compounds while generating minimal hazardous waste. A promising material used as an adsorbent was bagasse, a biomass byproduct abundantly available in Indonesia. Bagasse was composed primarily of lignocellulose, including cellulose, hemicellulose, and lignin. These components contributed to its porous structure and high carbon content, rendering it an excellent candidate as a base material for adsorbents [9]. The activation of bagasse with sodium hydroxide (NaOH) solution had been shown to enhance surface area, increase pore volume, and introduce active functional groups such as hydroxyl and carboxyl groups, thereby improving adsorption capacity [10].

In addition to biomass, bentonite served as a natural adsorbent characterized by high cation exchange capacity, substantial surface area, and excellent structural stability. The montmorillonite mineral content in bentonite played a crucial role in the effective adsorption of both organic and inorganic compounds [11, 12]. The combination of bagasse with bentonite held potential for producing composite materials with enhanced adsorption efficiency by leveraging the synergy between the porosity of the bioadsorbent and the structural stability provided by bentonite.

The application of sugarcane bagasse–bentonite composites and their NaOH-activated variants represented an effective strategy for reducing the peroxide value of used cooking oil. This approach not only enhanced the quality of recycled oil but also promoted the sustainable utilization of biomass and mineral waste within the framework of a circular economy. The primary objective of this study was to evaluate and compare the effectiveness of these composites in decreasing peroxide value, while also elucidating their adsorption mechanisms through FTIR, SEM, and EDX analyses.

2. Materials and Methods

2.1. Raw material.

Used cooking oil was collected from a local small-scale food vendor (UMKM) engaged in repeated frying processes. Sugarcane bagasse was used as the biochar precursor, while bentonite was employed as the supporting material for composite preparation.

2.2. Chemicals.

Some of the chemicals used for peroxide adsorption include Glacial Acetic Acid 100% (Merck), Chloroform 99.8% (Merck), Sodium Thiosulfate 0.1 N (Merck), Amylum 1% (Merck), and Potassium Iodide (Merck). In addition, NaOH 0.5 N (Merck) is used to activate the biochar before compositing.

2.3. Material preparation.

2.3.1. Bentonit.

To prepare the bentonite suspension, 250 g of commercially sourced bentonite was mixed with 2 l of distilled water and stirred for 10 minutes. The mixture was then allowed to settle for 24 hours. The supernatant was discarded, and the sediment was filtered and subsequently dried in an oven at 105°C for 3 hours. After drying, the bentonite was ground into a fine powder and passed through a 100-mesh sieve (0.149 mm) to obtain a uniform particle size. The processed bentonite was stored in a desiccator and an airtight container at room temperature to prevent moisture absorption.

2.3.2. Sugarcane bagasse biochar.

Sugarcane bagasse biomass was cut into pieces measuring approximately 5–10 cm in length and thoroughly washed with distilled water to remove impurities. The washed biomass was dried at 105°C for 12 hours. After drying, the biomass underwent pyrolysis at 250°C for 1 hour to produce biochar. The resulting biochar was ground and sieved to a particle size of 100 mesh (0.149 mm) and stored in a desiccator. The biochar was then activated using a sodium hydroxide (NaOH) solution at a ratio of 1:5 (biochar to NaOH 0.5 N) and allowed to stand for 24 hours [13]. Following activation, the biochar was washed until neutral pH was achieved, dried at 105°C for 2 hours, and stored in an airtight container at room temperature.

2.3.3 Biochar-bentonite composite.

Bentonite was mixed with distilled water at a ratio of 1:20 (bentonite to distilled water) and stirred for 20 minutes using a jar test apparatus. Biochar was then added to the bentonite suspension at a mass ratio of 1:1 and stirred for an additional 2 hours. The mixture was allowed to settle and subsequently filtered using a vacuum pump to separate the composite from the residual solution. The obtained composite was dried at 105°C for 2 hours and sieved through a 100-mesh sieve (0.149 mm). The composite was stored in a desiccator and an airtight container at room temperature.

2.4. Characterization analysis.

Both NaOH-activated and non-activated biochar–bentonite composites underwent characterization analyses using scanning electron microscopy (SEM), energy-dispersive X-ray spectroscopy (EDX), and Fourier transform infrared spectroscopy (FTIR). SEM-EDX analysis was conducted using a Hitachi FlexSEM 1000 equipped with AMETEK EDAX to examine surface morphology and elemental distribution. Functional groups were analyzed using FTIR (Agilent Technologies). In addition, the initial and final peroxide values were determined using iodometric titration in accordance with SNI 7709:2012.

2.5. Adsorption study.

The adsorption study was conducted by varying the adsorbent dose and treatment time. The effectiveness of peroxide number reduction (E) and the adsorption capacity (q) for each variation were calculated using Eqs. (1) and (2).

$$E\ (\%) = \frac{C_0 - C_1}{C_0} \text{x } 100 \qquad \text{Eq. 1}$$

where E is the removal efficiency (%); C_0 is the initial concentration before adsorption (mg/L); C_1 is the concentration after adsorption (mg/L)

$$q\left(\frac{mg}{g}\right) = \frac{(C_0 - C_1)\,V}{m} \qquad \text{Eq. 2}$$

where q is the adsorption capacity (mg/g); C_0 is the initial concentration before adsorption (mg/L); is the concentration after adsorption (mg/L); V is the volume of the solution; m is the mass of the adsorbent used (g)

2.5.1. Effect of different dosage adsorbent.

The adsorbent dosage was varied to determine the optimal amount for the adsorption of peroxide value from used cooking oil. In this experiment, 100 mL of used cooking oil was placed in a 250 mL beaker, and different masses of the biochar–bentonite composite (2, 4, 6, 8, and 10 g) were added. The mixture was stirred using a mixer at 250 rpm for 180 minutes at a temperature of 50°C. After the adsorption process was completed, the mixture was centrifuged to separate the adsorbent residue from the oil filtrate. The resulting filtrate was then used for peroxide value analysis.

2.5.2. Effect of treatment time.

The treatment time was varied to determine the optimal adsorption duration for the removal of peroxide value from used cooking oil. A total of 100 mL of used cooking oil was placed in a 250 mL beaker, and the biochar–bentonite composite was added. The mixture was stirred at 250 rpm for different time intervals of 30, 60, 90, 120, 150, and 180 minutes to ensure homogeneity. During the experiment, other parameters were kept constant, including an adsorbent dosage of 10 g and a temperature of 50°C. After the adsorption process, the mixture was centrifuged to separate the adsorbent residue from the oil filtrate. The obtained filtrate was subsequently analyzed to determine the peroxide value.

2.6. Peroxide value analysis.

Peroxide value analysis was conducted in accordance with SNI 7709:2019. A total of 5 g of used cooking oil was placed in a 250 mL Erlenmeyer flask, followed by the addition of 50 mL of a glacial acetic acid–chloroform mixture (3:2, v/v). After homogenization, 0.5 mL of potassium iodide (KI) solution was added, and the mixture was stirred again before adding 30 mL of distilled water. The sample was then titrated with 0.1 N sodium thiosulfate ($Na_2S_2O_3 \cdot 5H_2O$) solution until the yellow color nearly disappeared. Subsequently, 0.5 mL of a 1% starch indicator was added, and the titration was continued until the blue color completely disappeared. The analysis was performed in duplicate, and the volume of sodium thiosulfate consumed was recorded to calculate the peroxide value using Eq. (3):

$$PV\ \left(\frac{meqO_2}{kg}\right) = \frac{1000\ x\ N\ x\ (V_0 - V_1)}{W} \qquad \text{Eq. 3}$$

where N is the normality of the $Na_2S_2O_3$. $5H_2O$ solution (N); V_1 is the volume of sodium thiosulfate solution for titrating the sample (mL); V_0 is the volume of sodium thiosulfate solution for titrating the blank (mL); W is the weight of the sample (g).

3. Results and Discussion

3.1. Characterization analysis.

3.1.1. Scanning Electron Microscope-Energy Dispersive X-ray (SEM-EDX) analysis.

Surface morphology analysis was performed using SEM to examine the surfaces of the sugarcane bagasse–bentonite biochar composite (SBB) and the activated sugarcane bagasse–bentonite composite (ASBB). In addition, EDX analysis was conducted to identify and map the distribution of chemical elements on the surface of the solid materials. Figure 1(A) illustrates the Scanning Electron Microscopy (SEM) results of the SBB composite, showing that the biochar surface retained a relatively smooth texture with a porous structure that was not yet fully developed. At a magnification of 1000×, the pores appeared to be partially filled with bentonite particles adhering to the pore walls. This observation suggested that the mixing process resulted in a relatively uniform distribution of bentonite on the biochar surface. Such structural features indicated effective physical interaction between biochar and bentonite, leading to the formation of a stable and homogeneously distributed composite [13–15]. In contrast, Figure 1(B) presents the SEM analysis of the ASBB composite. The surface structure was noticeably rougher and more irregular, with more pronounced voids and cracks compared to the non-activated composite. The NaOH activation process facilitated the formation of new pores and increased the number of active sites on the biochar surface, thereby enhancing the interaction between biochar and bentonite and allowing bentonite particles to occupy the pore voids more effectively [17]. The presence of surface cracks further indicated an increase in specific surface area, which could significantly enhance the adsorption capacity of the composite [18].

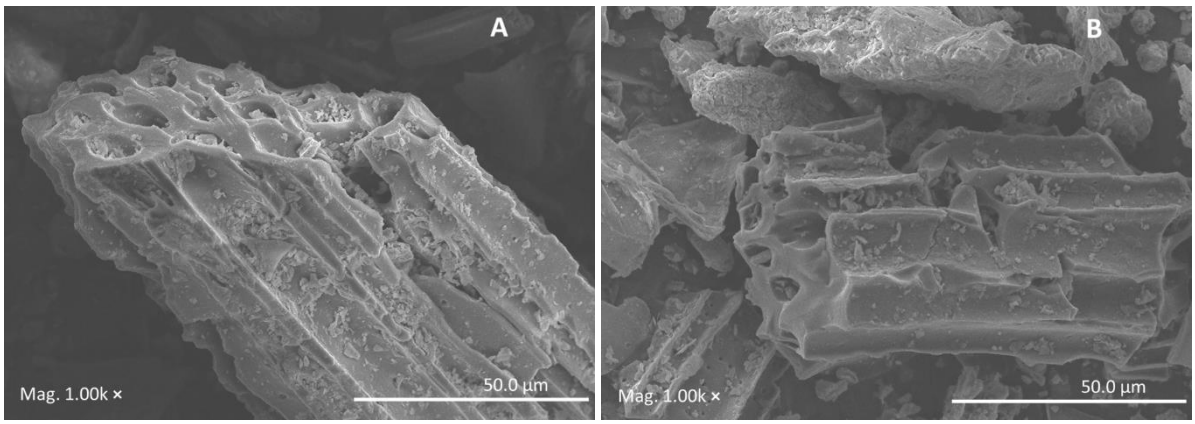

Figure 1. SEM analysis results SBB (A); ASBB (B).

Table 1 presents the elemental composition of the SBB composite, showing that carbon (C) accounted for 57.93% and oxygen (O) comprised 28.96%. In addition, mineral elements such as silicon (Si) at 9.51% and calcium (Ca) at 0.94% were detected, which are characteristic of bentonite. The predominance of carbon indicated that the biochar structure remained the

primary component of the composite, while the presence of mineral elements confirmed the successful incorporation of bentonite onto the biochar surface [19]. Aluminum (Al) was detected in trace amounts (0.87%), as it primarily resided within the interlayer structure of bentonite and was often masked by silicon and oxygen signals in the EDX analysis [20]. In contrast, the ASBB composite also exhibited dominant carbon and oxygen elements; however, NaOH activation resulted in a marked reduction in carbon content from 57.93% to 29.41%. This decrease was attributed to the removal of volatile carbon-containing compounds during the activation process [17]. Conversely, the relative concentrations of oxygen, silicon, aluminum, magnesium (Mg), and calcium increased due to pore expansion and the disruption of mineral bonds induced by NaOH treatment [21]. Furthermore, the presence of sodium (Na) as a residual element from the activation process contributed to an increased negative surface charge on the adsorbent, thereby enhancing electrostatic interactions with polar compounds during the adsorption process.

Table 1. Element composition in SBB and ASBB.

Item	SBB (%wt)	ASBB (%wt)
C	57.93	29.41
O	28.96	41.12
Si	9.51	17.02
Al	0.87	3.93
Mg	0.28	0.42
Ca	0.94	2.17
K	0.40	0.59
Fe	1.12	3.29
Na	-	2.04

3.1.2. Fourier-Transform Infrared Spectroscopy (FTIR) analysis.

Figure 2 illustrates the Fourier Transform Infrared (FTIR) spectra of the SBB composite (black line) and the ASBB composite (blue line). In the SBB spectrum, the broad band observed in the region of 3340–3390 cm^{-1} corresponded to O–H stretching vibrations, which were attributed to hydroxyl groups present in both bentonite and the lignocellulosic residues of biochar. The bands at 1580 cm^{-1} and 1423 cm^{-1} indicated the presence of aromatic C=C bonds and carboxylate ($–COO^–$) groups, respectively. Additionally, the band observed in the range of 1000–1050 cm^{-1} signified Si–O–Si and Si–O–Al stretching vibrations, indicating effective integration between the bentonite aluminosilicate framework and the oxygen-containing functional groups of the biochar [22]. This observation suggested that the bentonite structure remained stable and contributed to an increased number of active adsorption sites. In the ASBB spectrum, prominent bands at 3623 and 3339 cm^{-1} demonstrated an increase in the intensity of O–H groups, resulting from the NaOH activation process and indicating the formation of a more hydrophilic surface. The shift of the band from 1423 cm^{-1} to 1401 cm^{-1} signified the interaction of carboxylate ($–COO^–$) groups with sodium (Na^+) ions, leading to the formation of additional polar and charged active sites [23]. Peaks observed at 1006 and 872 cm^{-1} further confirmed the dominance of the Si–O–Si and Si–O–Al structures and suggested the formation of new functional groups due to modifications in the silicate framework. Overall, NaOH activation enhanced both the abundance and reactivity of hydroxyl and silicate groups, producing a more polar and reactive surface that ultimately improved the adsorption capacity for polar compounds present in used cooking oil.

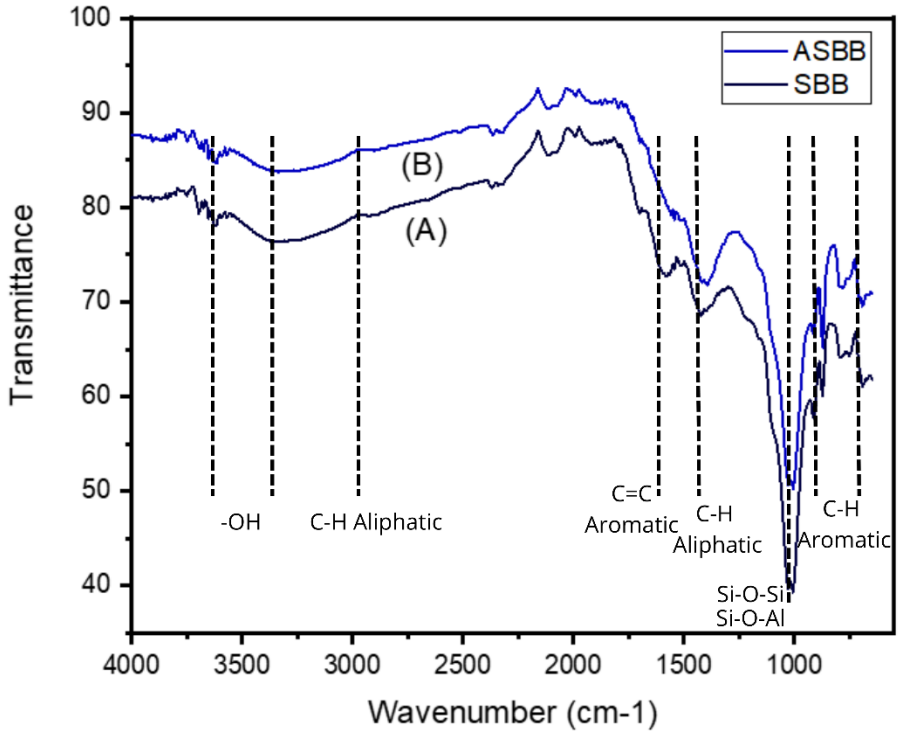

Figure 2. FTIR analysis results SBB (A); ASBB (B).

3.2. Effect of different dosage adsorbent.

An adsorbent dose ranging from 2 to 10 g was used to investigate the peroxide value reduction efficiency (E) and adsorption capacity (q) of the SBB and ASBB composites. All reported data represented the average values obtained from duplicate experiments. As shown in Figure 3, an increase in the adsorbent dose led to an increase in peroxide reduction efficiency. Initially, the peroxide value of the used cooking oil was 56.42 meq O_2/kg. Using the SBB composite, the reduction efficiency increased to 70.14%, whereas the ASBB composite achieved a higher efficiency of 82.33%. These results indicated that increasing the adsorbent dose provided more available active sites to interact with hydroperoxide groups [24, 25]. In contrast, as the adsorbent dosage increased, the specific adsorption capacity (q) decreased. At lower dosages, the active sites on the adsorbent were more accessible, allowing for greater peroxide adsorption per unit mass. However, at higher dosages, the available peroxide compounds became limited relative to the number of active sites, leading to partial site saturation and a reduction in adsorption capacity [26]. This adsorption behavior was consistent with the FTIR and SEM–EDX analyses, which supported the proposed mechanism through the identification of –OH, C=O, and Si–O–Si functional groups, as well as the increased presence of Si, Al, and Na elements in the ASBB composite, indicating the formation of additional active adsorption sites [27–30]. Although a higher adsorbent dosage enhanced the overall peroxide removal efficiency (E), it simultaneously reduced the adsorption capacity per unit mass. Similar trends were reported in previous studies on used cooking oil purification. Wardoyo's study demonstrated that the addition of 10% (b/v) papaya powder reduced the peroxide value by 52.16% after 5 days of agitation using a shaker, indicating that an increased adsorbent dosage improved peroxide removal efficiency [31]. Likewise, Marlina's research reported that the addition of 6 g of NaOH-activated cocoa powder to 72 mL of used cooking oil decreased the peroxide value

from 15.3 meq O_2/kg to 3.25 meq O_2/kg [32]. These findings were consistent with the present study, in which the ASBB composite exhibited superior performance due to NaOH activation, which enhanced pore structure and introduced reactive functional groups, thereby improving interactions with hydroperoxide compounds [18, 21].

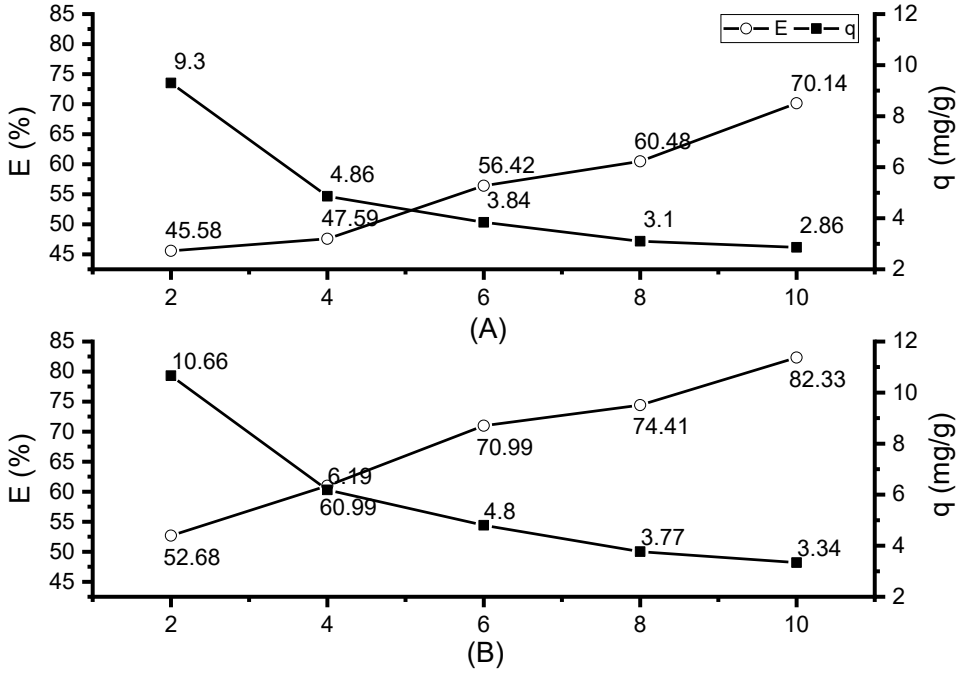

Figure 3. Peroxide value adsorption efficiency and adsorption capacity against different dosage adsorbent of SBB (A); ASBB (B).

As illustrated in Figure 4, peroxide adsorption onto SBB and ASBB occurred through a combination of pore filling and surface interactions. In the SBB composite, peroxide compounds were primarily adsorbed via physical interactions, including van der Waals forces and weak hydrogen bonding between hydroperoxide groups and surface –OH or –Si–OH functional groups. The porous structure observed in the SEM images facilitated the diffusion of peroxide molecules into internal pores, where adsorption predominantly occurred through pore filling [25, 33]. In contrast, the ASBB composite exhibited enhanced adsorption due to NaOH activation and bentonite incorporation, which increased surface alkalinity, pore accessibility, and the abundance of active sites. The presence of –OH, –Si–OH, and deprotonated $–COO^-$ groups, along with Na^+ counter ions, promoted stronger interactions such as hydrogen bonding and dipole–dipole interactions with peroxide molecules. These stronger interactions, combined with an improved pore structure, resulted in higher adsorption efficiency for ASBB compared to SBB [21, 34]. Overall, the adsorption mechanism involved a synergistic effect of pore filling and surface interactions, with ASBB demonstrating stronger and more effective peroxide binding.

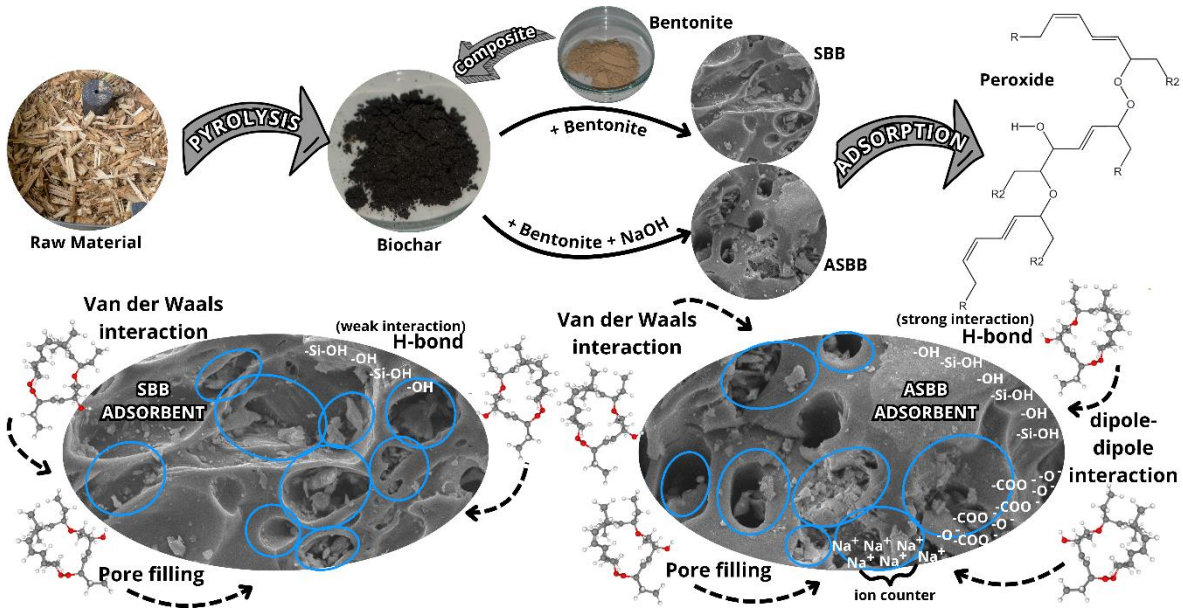

Figure 4. Adsorption mechanism of SBB and ASBB adsorbents.

3.3. Effect of treatment time.

Treatment time was a critical factor in determining the rate and quantity of peroxide molecules that interacted with the adsorbent surface. All reported data represented the average values obtained from duplicate experiments. As illustrated in Figure 5, the removal efficiency (E) of the SBB and ASBB composites increased with extended treatment time. During the initial 0 to 30 minutes, the increase in efficiency occurred rapidly because the adsorbent surface provided a large number of readily accessible active sites. However, after reaching 150 minutes, the increase in adsorption efficiency for the ASBB composite decelerated, indicating that the system was approaching adsorption equilibrium, in which most active sites had been occupied [35, 36]. In contrast, the SBB composite exhibited a more gradual increase in efficiency up to 180 minutes. This behavior was attributed to the absence of an activation treatment, which resulted in some pores remaining obstructed by residual organic materials from the pyrolysis process. Consequently, the penetration of peroxide compound molecules into the pores and the occupation of deeper adsorption sites required a longer contact time [37].

A similar trend was observed for the adsorption capacity (q), which showed a rapid increase at the initial stage due to a high concentration gradient between the oil phase and the adsorbent surface, followed by a slower increase and eventual stabilization as surface saturation was approached [38]. Across all treatment times, the ASBB composite consistently exhibited higher removal efficiency and adsorption capacity than the SBB composite. This improvement was attributed to NaOH activation, which enhanced pore development and increased the availability of reactive functional groups such as –O– and –Na–O, thereby strengthening interactions with peroxide compounds [18, 29, 39]. Comparable adsorption behavior was reported in previous studies [40], which demonstrated that biochar could be regenerated after each adsorption step and reused for up to five adsorption–desorption cycles with only a slight decrease in capacity. However, the regeneration and reusability of ASBB were not investigated in the present study, highlighting an important aspect that may serve as a novelty and direction for future research.

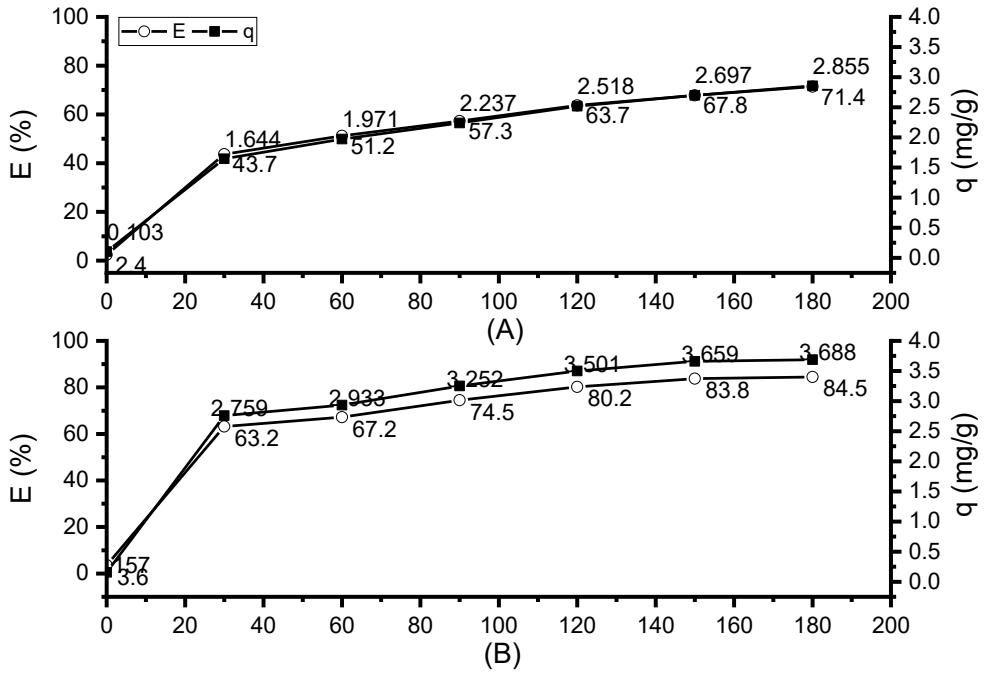

Figure 5. Peroxide value adsorption efficiency and adsorption capacity against treatment time on SBB (A); ASBB (B).

4. Conclusions

ASBB demonstrated superior effectiveness in reducing the peroxide value of used cooking oil compared to the non-activated composite. At an adsorbent dosage of 10 g, ASBB reduced the peroxide value by up to 82.33%, achieving a maximum efficiency of 84.5% after 180 minutes of contact time. The gradual stabilization of adsorption efficiency and capacity at prolonged treatment times indicated that equilibrium had been attained due to the saturation of available active sites. The enhanced performance of ASBB was attributed to NaOH activation, which improved the pore structure and increased the availability of reactive functional groups, thereby strengthening interactions with peroxide compounds. Compared with similar bio-based adsorbents reported in previous studies, the ASBB composite exhibited competitive adsorption performance, highlighting its practical potential as a low-cost and effective adsorbent for laboratory-scale purification of used cooking oil.

Acknowledgements

The author gratefully acknowledges the Water Treatment Technology Laboratory (Laboratorium Teknologi Pengolahan Air), Department of Environmental Engineering, Faculty of Civil, Environmental and Geo Engineering, Institut Teknologi Sepuluh Nopember for providing the facilities and support to conduct this research.

Data Availability

Data available upon request.

Author Contribution

Avissa Auryn Wijayanti: conceptualization, methodology, data collection, data analysis, and writing. Adhi Yuniarto: conceptualization, methodology, data analysis, writing and supervision. Indah Nurhayati: conceptualization, writing, supervision and funding. Sagita Rochman: methodology and supervision.

Competing Interest

The authors declarethat there is no conflict of interest.

References

[1] Viantini, F.; Yustinah. (2015). Pengaruh Teperatur pada Proses Pemurnian Minyak Goreng Bekas dengan Buah Mengkudu. *Konversi*, *4*(2), 53–62. https://doi.org/10.1007/978-94-007-5653-3_35.

[2] Chairgulprasert, V.; Madlah, P. (2018). Removal of Free Fatty Acid from Used Palm Oil by Coffee Husk Ash. *Science and Technology Asia*, *23*(3), 1–9. https://doi.org/10.14456/scitechasia.2018.18.

[3] Husnah, H.; Nurlela, N. (2020). Analisa Bilangan Peroksida Terhadap Kualitas Minyak Goreng Sebelum dan Sesudah Dipaka Berulang. *Jurnal Redoks*, *5*(1), 65–71. https://doi.org/10.31851/redoks.v5i1.4129.

[4] Burhan, A. H.; Rini, Y. P.; Faramudika, E.; Widiastusi, R. (2018). Penetapan Angka Peroksida Minyak Goreng Curah Sawit Pada Penggorengan Berulang Ikan Lele. *Jurnal Pendidikan Sains (Jps)*, *6*(2), 48. https://doi.org/10.26714/jps.6.2.2018.48-53.

[5] Kumar, A.; Bhayana, S.; Singh, P. K.; Tripathi, A. D.; Paul, V.; Balodi, V.; Agarwal, A. (2025). Valorization of Used Cooking Oil: Challenges, Current Developments, Life Cycle Assessment and Future Prospects. *Discover Sustainability*, *6*, 119. https://doi.org/10.1007/s43621-025-00905-7.

[6] Gusti, U. A.; Surtikanti, H. K. (2024). Analisis Limbah Minyak Jelantah Hasil Penggorengan Pelaku UMKM di Kelurahan Gegerkalong Kota Bandung. *Rekayasa Hijau: Jurnal Teknologi Ramah Lingkungan*, *8*, 263–272. https://doi.org/10.26760/jrh.v8i3.263-272.

[7] Huang, L.; Ye, J.; Jiang, K.; Wang, Y.; Li, Y. (2021). Oil Contamination Drives the Transformation of Soil Microbial Communities: Co-occurrence Pattern, Metabolic Enzymes and Culturable Hydrocarbon-degrading Bacteria. *Ecotoxicology and Environmental Safety*, *225*. https://doi.org/10.1016/j.ecoenv.2021.112740.

[8] Priskila, G.; Darmawan, P. (2022). Analisis Bilangan Peroksida dan Asam Lemak Bebas pada Minyak Goreng Curah Tidak Bermerek di Pasar Tradisional. *Jurnal Kimia Dan Rekayasa*, *3*(1), 21–26. https://doi.org/10.31001/jkireka.v3i1.41.

[9] Amalina, F.; Syukor Abd Razak, A.; Krishnan, S.; Sulaiman, H.; Zularisam, A. W.; Nasrullah, M. (2022). Advanced Techniques in The Production of Biochar from Lignocellulosic Biomass and Environmental Applications. *Cleaner Materials*, *6,* 100137. https://doi.org/10.1016/j.clema.2022.100137.

[10] Yogalakshmi, K. N.; Poornima, D. T.; Sivashanmugam, P.; Kavitha, S.; Yukesh, K. R.; Varjani, S.; AdishKumar, S.; Kumar, G.; Rajesh, B. J. (2022). Lignocellulosic Biomass-Based Pyrolysis: A Comprehensive Review. *Chemosphere*, *286*(P2), 131824. https://doi.org/10.1016/j.chemosphere.2021.131824.

[11] Al-Hammood, A. A.; Frayyeh, Q. J.; Abbas, W. A. (2021). Raw Bentonite as Supplementary Cementitious Material - A Review. *Journal of Physics: Conference Series*, *1795*, 012018. https://doi.org/10.1088/1742-6596/1795/1/012018.

[12] Rana, M. S.; Kim, S. (2024). Bentonite in Korea: A Resource and Research Focus for Biomedical and Cosmetic Industries. *Materials*, *17*(9), 1982. https://doi.org/10.3390/ma17091982.

[13] Ifa, L.; Syarif, T.; Sartia, S.; Juliani, J.; Nurdjannah, N.; Kusuma, H. S. (2022). Techno-economics of Coconut Coir Bioadsorbent Utilization on Free Fatty Acid Level Reduction in Crude Palm Oil. *Heliyon*, *8*(3), e09146. https://doi.org/10.1016/j.heliyon.2022.e09146.

[14] Adeniyi, A. G.; Sanusi, S. K.; Abdulkareem, S. A.; Ighalo, J. O.; Onifade, D. V. (2020). Thermochemical Co-conversion of Sugarcane Bagasse-LDPE Hybrid Waste into Biochar. *Arabian Journal for Science and Engineering*, *46,* 6391–6397. https://doi.org/10.1007/s13369-020-05119-9.

[15] Sathyabama, K.; Firdous, S. (2025). Effect of Pyrolysis Temperature on the Physicochemical Properties and Structural Characteristics of Agricultural Wastes-Derived Biochar [Research-article]. *ACS Omega*, *10*, 37013–37024. https://doi.org/10.1021/acsomega.5c00120.

[16] Tomczyk, A. (2020). Biochar physicochemical properties: pyrolysis temperature and feedstock kind effects. *Reviews in Environmental Science and Bio/Technology*, *19*(1), 191–215. https://doi.org/10.1007/s11157-020-09523-3.

[17] Premchand, P.; Demichelis, F.; Galletti, C.; Chiaramonti, D. (2024). Enhancing Biochar Production: A Technical Analysis of The Combined Influence of Chemical Activation (KOH and NaOH) and Pyrolysis Atmospheres. *Journal of Environmental Management*, *370*, 123034. https://doi.org/10.1016/j.jenvman.2024.123034.

[18] Valenga, M. G. P.; Gevaerd, A.; Marcolino-junior, L. H.; Bergamini, F. (2024). Biochar from sugarcane bagasse: Synthesis, characterization, and application in an electrochemical sensor for copper (II) determination. *Biomass and Bioenergy*, *184*, 107206. https://doi.org/10.1016/j.biombioe.2024.107206.

[19] Rupngam, T.; Udomkun, P.; Boonupara, T. (2025). Contrasting Pre- and Post-Pyrolysis Incorporation of Bentonite into Manure Biochar: Impacts on Nutrient Availability, Carbon Stability, and Physicochemical Properties. *Agronomy*, *15*, 2015. https://doi.org/10.3390/agronomy15082015.

[20] Newton, A. G.; Kwon, K. D.; Cheong, D. (2016). Edge Structure of Montmorillonite from Atomistic Simulations. *Minerals*, *6*, 25. https://doi.org/10.3390/min6020025.

[21] Lee, Y. G.; Shin, J.; Kwak, J.; Kim, S.; Son, C.; Cho, K. H.; Chon, K. (2021). Effects of NaOH Activation on Adsorptive Removal of Herbicides by Biochars Prepared from Ground Coffee Residues. *Energies*, *14*(5), 1297. https://doi.org/10.3390/en14051297.

[22] Hakim, M. S.; Iqbal, R. M.; Adany, F.; Putra, R.; Nitriany, I.; Telaumbanua, I. S.; Sitorus, R. U.; Dewi, R. K. (2024). A Review on Development of Porous Aluminosilicate-Based Zeolite Adsorbent for Heavy Metal Pollution Treatment. *Jurnal Sains Materi Indonesia (JUSAMI)*, *25*(2), 85–99. https://doi.org/10.55981/jsmi.2024.1076.

[23] Hisbullah; Kana, S.; Faisal, M. (2022). Characterization of Physically and Chemically Activated Carbon Derived from Palm Kernal Shells. *International Journal of Geomate*, *23*(97), 203–210.

[24] El-nemr, M. A.; Nemr, A. El; Hassaan, M. A.; Ragab, S.; Tedone, L.; Mastro, G. De; Pantaleo, A. (2022). Microporous Activated Carbon from Pisum sativum Pods Using Various Activation Methods and Tested for Adsorption of Acid Orange 7 Dye from Water. *Molecules*, *27, 4*840. https://doi.org/10.3390/molecules27154840.

[25] Jha, S.; Gaur, R.; Shahabuddin, S. (2023). Biochar as Sustainable Alternative and Green Adsorbent for the Remediation of Noxious Pollutants: A Comprehensive Review. *Toxics*, *11*, 117. https://doi.org/10.3390/toxics11020117

[26] Zain, N. B. M.; Salleh, N. J.; Hisamuddin, N. F.; Hashim, S.; Abdullah, N. H. (2022). Adsorption of Phosphorus Using Cockle Shell Waste. *Industrial and Domestic Waste Management*, *2*(1), 30–38. https://doi.org/10.53623/idwm.v2i1.81.

[27] Irawan, D.; Wijayanti, W.; Wahyudi, S.; Wardana, I. N. G. (2025). Modification effects of Na-bentonite catalyst with organic compounds increasing hydrogen production from biomass

pyrolysis. *Case Studies in Chemical and Environmental Engineering*, *11*, 101206. https://doi.org/10.1016/j.cscee.2025.101206.

[28] Suzuki, R. (2024). Effect of Adding Bentonite to Porous Silica via the Sol − Gel Method. *ACS Omega*, *9,* 10577–10582. https://doi.org/10.1021/acsomega.3c08832.

[29] Jedynak, K.; Charmas, B. (2024). Adsorption properties of biochars obtained by KOH activation. *Adsorption*, *30*(2), 167–183. https://doi.org/10.1007/s10450-023-00399-7.

[30] Faggiano, A.; Cicatelli, A.; Guarino, F.; Castiglione, S.; Proto, A.; Fiorentino, A.; Motta, O. (2025). Optimizing CO2 capture: Effects of chemical functionalization on woodchip biochar adsorption performance. *Journal of Environmental Management*, *380*, 125059. https://doi.org/10.1016/j.jenvman.2025.125059.

[31] Wardoyo, F. A. (2018). Penurunan Bilangan Peroksida Pada Minyak Jelantah Menggunakan Serbuk Daun Pepaya. *Jurnal Pangan Dan Gizi*, *8*(2).

[32] Marlina, R.; Oktasari, A.; Rohmatullaili, R. (2022). Utilization of Adsorbent Cocoa Shell For Purification of Used Cooking Oil. *Stannum: Jurnal Sains dan Terapan Kimia*, *4*(1), 6–12. https://doi.org/10.33019/jstk.v4i1.2638.

[33] Zafeer, M. K.; Menezes, R. A.; Venkatachalam, H.; Bhat, K. S. (2024). Sugarcane Bagasse-based Biochar and Its Potential Applications: A Review. *Emergent Materials*, *7*(1), 133–161. https://doi.org/10.1007/s42247-023-00603-y.

[34] Murtaza, G.; Ahmed, Z.; Valipour, M.; Ali, I.; Usman, M.; Iqbal, R.; Zulfiqar, U.; Rizwan, M. (2024). Recent trends and economic significance of modified / functionalized biochars for remediation of environmental pollutants. *Scientific Reports, 14,* 217. https://doi.org/10.1038/s41598-023-50623-1.

[35] Kouadio, L. M.; Larregieu, M.; Tillous, K. E. N.; Sei, J.; Tison, Y.; Parat, C.; Pannier, F.; Martinez, H. (2024). Evaluation of the capacity of Ivory Coast clay to depollute water contaminated by Hg, Pb, Cd and As. *South Africa Journal of Chemistry*, *177*, 170–177. https://doi.org/10.17159/0379-4350/2024/v78a23.

[36] Anuar, F. I.; Hadibarata, T.; Muryanto; Yuniarto, A.; Priyandoko, D.; Sari, A. A. (2019). Innovative Chemically Modified Bioadsorbent for Removal of Procion Red. *International Journal of Technology*, *10*(4), 776–786. https://doi.org/10.14716/ijtech.v10i4.2398.

[37] Hamid, S. B. A.; Chowdhury, Z. Z.; Zain, S. M. (2014). Base Catalytic Approach: A Promising Technique for the Activation of Biochar for Equilibrium Sorption Studies of Copper, Cu(II) Ions in Single Solute System. *Materials*, *7*, 2815–2832. https://doi.org/10.3390/ma7042815.

[38] Biyikoğlu, M. (2025). Innovative approaches in wastewater treatment: kinetic and isotherm investigation of dye adsorption on sulfur-modified PET fibers. *Research on Chemical Intermediates*, *51*(6), 3281–3299. https://doi.org/10.1007/s11164-025-05599-0.

[39] Arumugham, T.; Yuniarto, A.; Abdullah, N.; Yuzir, A.; Kamyab, H.; Pa, N. F. C.; Rezania, S.; Hatta, M. N. M. (2023). Preparation and Characterisation of Porous Activated Carbon Using Potassium Hydroxide Chemical Activation with Ultrasonic Association. *Biomass Conversion and Biorefinery*, *15*(19), 26071–26083. https://doi.org/10.1007/s13399-023-05201-w.

[40] Ma, H.; Xu, Z.; Wang, W.; Gao, X.; Ma, H. (2019). Adsorption and regeneration of leaf-based biochar for p-nitrophenol adsorption from aqueous solution. *RSC Advances*, *9*, 39282–39293. https://doi.org/10.1039/c9ra07943b.